Remediation and Control Technologies

Ozonation of Microcystins: Kinetics and Toxicity Decrease

Min-Sik Kim, and Changha Lee

Environ. Sci. Technol., **Just Accepted Manuscript** • DOI: 10.1021/acs.est.8b06645 • Publication Date (Web): 06 May 2019

Ozonation of Microcystins: Kinetics and Toxicity Decrease

Min Sik Kim, Changha Lee*

School of Chemical and Biological Engineering, Institute of Chemical Process (ICP), Seoul National University, 1 Gwanak-ro, Gwanak-gu, Seoul 08826, Republic of Korea

Submitted to

Environmental Science and Technology

*Corresponding author.

Tel.: +82–2–880–8630, Fax: +82–2–888–7295, E–mail: leechangha@snu.ac.kr

TOC/Abstract art

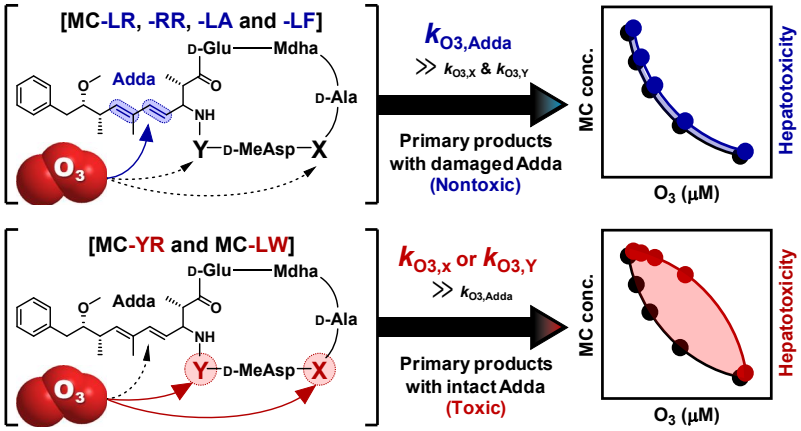

ABSTRACT

The ozonation of six microcystins (MCs) (MC-LR, -RR, -LA, -LF, -YR, and -LW) was investigated with a focus on the kinetics and decrease in toxicity. Second-order rate constants for the reactions of the six MCs with O_3 and $^{\bullet}OH$ ($k_{O3,MC}$ and $k_{\bullet OH,MC}$) ranged from 7.1×10^5 to 6.1×10^6 M^{-1} s^{-1} ($k_{O3,MC}$) and from 1.2×10^{10} to 1.8×10^{10} M^{-1} s^{-1} ($k_{\bullet OH,MC}$), respectively, at pH 7.2 and 20°C. The activation energies were calculated to be 21.6–34.5 kJ mol^{-1} and 11.6–13.1 kJ mol^{-1} for the $k_{O3,MC}$ and $k_{\bullet OH,MC}$, respectively. The rate constants did not show an important pH-dependency, except for $k_{O3,MC\text{-}YR}$, which increased at pH > 7. A kinetic model using the determined rate constants and the measured exposures of O_3 and $^{\bullet}OH$ was able to precisely predict the removal of MCs in natural waters. The hepatotoxicities of MCs were decreased by ozonation; the toxicities of the four MCs (MC-LR, -RR, -LA, and -LF) decreased nearly concurrently with decreases in their concentrations. However, MC-YR and MC-LW showed a gap between concentration and toxicity due to the incomplete destruction of the Adda moiety (a key amino acid expressing the hepatotoxicity of MCs). A product study using liquid chromatography-mass spectrometry identified a number of oxidation products with an intact Adda moiety produced by the ozonation of MC-YR and MC-LW.

INTRODUCTION

Microcystins (MCs), released by various genera of cyanobacteria (e.g., *Microcystis*, *Anabaena*, *Nodularia*, *Oscillatoria*, *Nostoc*, etc.), are the most frequently found cyanotoxins in eutrophied water bodies.[1,2] MCs are known to be acute hepatotoxins that inhibit protein phosphatases such as PP1 and PP2A, and to induce liver cancer by long-term exposure through drinking water.[3–6] The median lethal dose of MC-LR (the most common MC) is similar to that of *Crotalus atrox* venom (one of the reference snake venoms) (i.e., $LD_{50,MC\text{-}LR}$ = 50 μg kg^{-1} and $LD_{50,C.\ atrox}$ = 56 μg kg^{-1} in mice).[7,8] One historical case of MC poisoning that took place in Caruaru, Brazil in 1996, resulted in 60 human fatalities.[9,10] Because of the health risks caused by MCs, the World Health Organization (WHO) has set a provisional drinking water guideline value of 1 μg L^{-1} for MC-LR.[11]

MCs are cyclopeptides which consist of seven amino acids: a unique β-amino acid known as Adda ((2S,3S,8S,9S)-3-amino-9-methoxy-2,6,8-trimethyl-10-phenyldeca-4,6-dienoic acid), *N*-methyldehydroalanine (Mdha), three D-amino acids (alanine (Ala), glutamic acid (Glu) and erythro-β-methylaspartic acid (MeAsp)), and two variable L-amino acids (X and Y).[12] Different MC congeners exist depending on the L-amino acids in the X and Y positions (exceptionally, a few MCs have structural modifications in Mdha and MeAsp moieties).[13] Among the more than 100 MC congeners that have been reported to date, MC-LR, -RR, -LA, -LF, -YR, and -LW are those most commonly detected in aquatic environments.[14–16]

Ozonation has been widely applied in drinking water treatment plants for the oxidation of organic contaminants and disinfection of pathogens. Molecular ozone (O_3) is a reactive oxidant, capable of oxidizing various organic compounds.[17] In addition, O_3 decays to the more reactive hydroxyl radical which less selectively oxidizes a broad spectrum of organic compounds with high second-order rate constants.[18] The oxidation of organic contaminants by ozonation is governed by reactions with O_3 and $^{\bullet}OH$. The contributions of O_3 and $^{\bullet}OH$ are determined by the rate constants and oxidant

exposures; the reaction of O_3 generally dominates over that of •OH when the second-order rate constant for the reaction of O_3 with the organic compound exceeds 100 M^{-1} s^{-1} in natural waters.[19]

The ozonation of MCs has been investigated by several studies.[20–27] It has been shown that ozonation is very effective in oxidizing MCs, because the MC structure contains several alkene groups that are vulnerable to attack from O_3.[24,28] Previous studies on the ozonation of MCs have dealt with various aspects, including the reaction kinetics[22,24,25], effects of treatment conditions and water quality parameters[20–25], oxidation mechanism[25–27], and toxicity changes[23,26]. However, in spite of these studies, certain points of information regarding the ozonation of MCs still need to be elucidated. Basically, most previous studies have focused on MC-LR, and limited information is available for other important MC congeners. In terms of kinetics, the second-order rate constants for reactions with O_3 and •OH ($k_{O3,MC}$ and $k_{•OH,MC}$) as well as their activation energies (E_a) are largely unknown for MCs, except for MC-LR; even the reported $k_{O3,MC\text{-}LR}$ values are discrepant in the literature (from 3.8×10^4 to 4.1×10^5 M^{-1} s^{-1} [22,24,25]). The information on toxicity changes is also limited for the ozonation of different MCs. It has been reported that the hepatotoxicities of MC-LR, -RR, and -LA decreased to the same tendency as the concentration decreased.[23,26] However, different observations may be obtained for other MCs; indeed, some MCs show different trends in decreases of concentration and toxicity during ozonation (found in this study).

In this study, the oxidation of six major MCs (i.e., MC-LR, -RR, -LA, -LF, -YR, and -LW) by ozonation was investigated with a focus on the kinetics and toxicity decrease. The objectives of this study were (i) to obtain valid kinetic data regarding the reactions of select MCs with O_3 and •OH, (ii) to assess changes in toxicity during the ozonation of MCs, and (iii) to elucidate the oxidation mechanisms of MCs in relation to the toxicity decrease. For these purposes, the $k_{O3,MC}$ and $k_{•OH,MC}$ values were determined at various pHs and temperatures, and E_a values for the rate constants were calculated as well. A kinetic model using the determined rate constants was tested to predict the removal of MCs in natural waters. The PP2A activity was monitored to assess the hepatotoxicities of

MC solutions during ozonation. In addition, the oxidation products of MCs were analyzed by liquid chromatography-mass spectrometry (LC/MS).

MATERIALS AND METHODS

Reagents. All chemicals were of reagent grade and used without further purification (refer to the Supporting Information (SI), Text S1 for details). Six isolated MCs (i.e., MC-LR, -RR, -LA, -LF, -YR, and -LW; ≥95%) were purchased from Enzo Life Sciences Inc. All solutions were prepared using deionized (DI) water (>18.2 MΩ cm, Millipore, U.S.A.). O_3 stock solutions (ca. 30 mg L^{-1}) were produced by sparging O_3-containing oxygen gas (generated by an O_3 generator, Lab-II, Ozonetech, Korea) through DI water in an ice bath.

Determination of $k_{O3,MC}$. The $k_{O3,MC}$ values were determined by competition kinetics (CK) using cinnamic acid (CA) as a reference compound.[24] Since the literature shows discrepancies between the reported values of the second-order rate constant for the reaction of CA with O_3 ($k_{O3,CA}$) (3.8×10^5 M^{-1} s^{-1} [29], 7.6×10^5 M^{-1} s^{-1} [30], and 1.2×10^6 M^{-1} s^{-1} [31]), the $k_{O3,CA}$ values determined in this study were used. The $k_{O3,CA}$ values at different pHs and temperatures were determined by measuring the decrease of CA concentration in the presence of excess O_3, using stopped-flow spectrometry (SFS) (SFM-4000, Bio-Logic, France). Details for the determination of $k_{O3,CA}$ are described in SI Text S2, Table S1, S2, and Figures S1–S4.

All of the CK experiments for the determination of $k_{O3,MC}$ were performed with 10 mL solutions in a 25 mL-beaker containing 0.1 μM target MC, 0.1 μM CA, 5 mM *tert*-butanol (*t*-BuOH, a •OH scavenger), and a pH buffer. The solution pH was controlled by 1 mM phosphate (for pH 6.2–7.1) and borate (for pH 8–9) buffers. The reaction temperature was adjusted to the desired value by water circulation systems equipped with a probe type chiller (TC45E-F, Huber Co., Germany) (for 4–20°C) and a water bath heater (for 25–33°C). The reactions were initiated by injecting an aliquot

of O_3 stock solution into the pre-equilibrated reaction solutions under vigorous stirring. At least six CK experiments at different O_3 doses (0.025–0.25 μM) were conducted so as to complete a slope in a CK plot (refer to SI Figure S5).

Determination of $k_{\bullet OH,MC}$. The UV/H_2O_2 system was employed to generate $^{\bullet}$OH for the experiments. The CK method using *para*-chlorobenzoic acid (*p*CBA) as a reference compound was used to determine $k_{\bullet OH,MC}$; the second-order rate constant of *p*CBA with $^{\bullet}$OH ($k_{\bullet OH,pCBA}$) is known to be 5.0×10^9 M^{-1} s^{-1} at pH 6–9.4.[32] In order to help obtain the $k_{\bullet OH,MC}$ values at different temperatures, the temperature-dependency of $k_{\bullet OH,pCBA}$ (unknown in literatures) was determined in this study. Details of the determination of the temperature-dependent $k_{\bullet OH,pCBA}$ are described in SI Text 3 and Figure S6.

All of the CK experiments were performed with 20 mL solutions in a 30 mL quartz reactor placed in a dark chamber equipped with 4 W low-pressure mercury lamps (λ_{max} = 254 nm, Philips, U.S.A.) (SI Figure S7a). The incident light intensity of this setup was determined to be 1.27×10^{-6} Einstein s^{-1} L^{-1} by ferrioxalate actinometry (SI Figure S8).[33] The reaction solution contains 0.1 μM target MC, 0.1 μM *p*CBA, 1 mM buffer, and 1 mM H_2O_2. The initial pH and temperature were adjusted to the desired values in the same manner as described above for the $k_{O3,MC}$. The reaction was initiated by UV illumination and proceeded for 70 s. Samples (250 μL) were withdrawn every 10 s for analysis. Possible errors due to the direct UV photolysis of the target MC (the UV photolysis of *p*CBA was negligible) were corrected by control experiments without H_2O_2 (refer to SI Text S4 and Figures S7–S9 for details). All of the CK experiments for $k_{\bullet OH,MC}$ were carried out at least in duplicate, and the average values with standard deviations were presented.

Natural Water Samples. Two natural water samples were obtained from the Maegok drinking water treatment plant in Daegu and from lake Gamakin in Ulsan, Korea. The natural waters were filtered

with a 0.45 μm filter and stored at 4°C. The water quality parameters of natural water samples are summarized in SI (Table S3).

Analytical Methods. MCs were measured using rapid separation liquid chromatography (RSLC) (UltiMate 3000, Dionex, U.S.A.) with UV absorbance detection at 222 nm (for MC-LF) and 238 nm (for other MCs). The chromatographic separation was performed on an Acclaim™ C18 column (2.1 mm × 50 mm, 2.2 μm, 120 Å; Thermo Fisher Scientific, U.S.A.) using a mixture of 0.05% trifluoroacetic acid and methanol as eluent at a flow rate of 0.3 mL min^{-1}. The methanol contents in the mobile phase were 60% for MC-RR, -LR, and -YR and 70% for MC-LF, -LW, and -LA. The oxidation products of MCs were analyzed by RSLC coupled with a Q Exactive™ Quadrupole-Orbitrap Mass Spectrometer (Thermo Fisher Scientific, U.S.A.) (LC/MS). Details about the LC/MS analysis are provided in SI Text S5. CA, *p*CBA, and benzoic acid were also analyzed by RSLC with UV absorbance detection at 280, 230, and 254 nm, respectively.

The hepatotoxicities of MC solutions (untreated and treated by ozonation) was analyzed by the PP2A activity assay using a MicroCystest kit (ZEU Inmunotec, Spain). For the assay, the linear range in which the inhibition of PP2A activity is clearly observed was 0.25–2.5 nM as MC-LR. Samples were appropriately diluted so as to yield readings within this range. The relative inhibition of PP2A activity ([PP2A activity of DI water – PP2A activity of sample] / PP2A activity of DI water × dilution factor) was used as an indicator to represent the hepatotoxicity.

The decrease of O_3 in natural water experiments was measured by SFS (refer to SI Text S6 and Figure S10 for details). The concentration of dissolved organic carbon (DOC) was measured using a TOC analyzer (TOC-V_{CPH}, Shimadzu, Japan).

RESULTS AND DISCUSSION

Kinetics for the Reactions of MCs with O_3. In order to assess the reactivity of the six select MCs with O_3 at circumneutral pH range, $k_{O3,MC}$ values were determined with varying pH (6.2–9.0) and temperature (4–33°C) (SI Figures S11a and S11b). The $k_{O3,MC}$ values were calculated from the slopes of the CK plots (SI Figures S12 and S13) using pre-determined $k_{O3,CA}$ values ($k_{O3,CA(HA)}$ = 5.8 × 10^4 M^{-1} s^{-1} and $k_{O3,CA(A-)}$ = 7.5 ± 0.4 × 10^5 M^{-1} s^{-1}; refer to SI Tables S1, S2, Figures S3 and S4) as references. The determined $k_{O3,MC}$ values at pH 7.2 and 20°C were very similar (7.1–8.9 × 10^5 M^{-1} s^{-1}), except for MC-LW ($k_{O3,MC-LW}$ = 6.1 × 10^6 M^{-1} s^{-1}). The larger rate constant observed for MC-LW is due to the high reactivity of the tryptophan moiety (located in the Y position of MC-LW; refer to Figure 1) with O_3; the second-order rate constant of tryptophan with O_3 is known as 7 × 10^6 M^{-1} s^{-1} [34]).

Regarding $k_{O3,MC-LR}$, the value determined in this study was higher than those reported in previous studies (refer to Table 1). The very low literature values of $k_{O3,MC-LR}$ determined by SFS (3.4 × 10^4 M^{-1} s^{-1} [22] and 6.8 × 10^4 M^{-1} s^{-1} [25]) are believed to be underestimated, because the background UV absorbance of O_3 was not corrected when monitoring the UV absorbance change in the SFS experiments; indeed, our SFS experiments with a proper correction of O_3 absorbance obtained a $k_{O3,MC-LR}$ value of 8.0 × 10^5 M^{-1} s^{-1} (SI Figure S14), which is comparable to the value determined by the CK method (8.5 × 10^5 M^{-1} s^{-1} in Table 1). The $k_{O3,MC-LR}$ value determined by Onstad et al. (4.1 × 10^5 M^{-1} s^{-1} [24]) was approximately two-fold lower than ours, despite the fact that the same experimental method (the CK method using CA as a reference) was used. This discrepancy results from the difference in the reference $k_{O3,CA}$ values used in the two studies, as the study by Onstad et al. used a $k_{O3,CA}$ of 3.8 × 10^5 M^{-1} s^{-1}, while this study used a $k_{O3,CA}$ of 7.5 × 10^5 M^{-1} s^{-1} (determined in this study, SI Figure S4, and consistent with the most recently reported value of $k_{O3,CA}$, 7.6 × 10^5 M^{-1} s^{-1} [30]). Overall, the rate constants of two studies agree well and the difference of about a factor of 2 can be explained by a similar difference in rate constants for the reference

compound CA. This illustrates that the values of second-order rate constants for the reference compounds is decisive for the CK method.

Most of the $k_{O3,MC}$ values did not show any pH-dependency over pH 6.2–9.0, except for $k_{O3,MC\text{-}YR}$ (SI Figure S11a). The $k_{O3,MC\text{-}YR}$ value increased with increasing pH due to the deprotonation of the phenolic group in the tyrosine moiety ($-C_6H_5OH \rightarrow -C_6H_5O^-$, p$K_a$ = 9.9); the second-order rate constant for the reaction of phenolate with O_3 is much higher than that of phenol ($k_{O3,phenolate}$ = 1.4 × 10^9 M^{-1} s^{-1} > $k_{O3,phenol}$ = 1.3 × 10^3 M^{-1} s^{-1} [35]). This also indicates that the phenolic group in the tyrosine moiety of MC-YR is an important primary oxidation site by O_3.

The temperature-dependency of $k_{O3,MC}$ was examined in the temperature range of 4–33°C (SI Figure S11b). The $k_{O3,MC}$ values generally increased by 0.5 to 2.1-fold when the temperature was elevated from 4 to 33°C. The E_a values for the reactions of MCs with O_3 were calculated to be 21.6–34.5 kJ mol^{-1} (Table 1) from the slope of the Arrhenius plot (SI Figure S15a), which are similar to the reported E_a values for the reactions of other alkene containing compounds with O_3.[30,36] These E_a values indicate that the $k_{O3,MC}$ values vary by 0.7 to 2.1-fold in the range of temperature, at which the cyanobacterial blooms generally take place (10.5–34.0°C).[37]

Kinetics for the Reactions of MCs with •OH. The $k_{•OH,MC}$ values were determined at different pHs (6.2–9.0) and temperatures (4–33°C) (SI Figures S11c and S11d; refer to SI Figures S16 and S17 for their CK plots). All of the determined rate constants were quite similar to each other (1.2–1.6 × 10^{10} M^{-1} s^{-1}) and showed no pH-dependency, which reflects the lower selective reactivity of •OH. The $k_{•OH,MC\text{-}LR}$, $k_{•OH,MC\text{-}RR}$, $k_{•OH,MC\text{-}LA}$, and $k_{•OH,MC\text{-}YR}$ values determined in this study are consistent with the literature values (refer to Table 1).[24,38,39] The $k_{•OH,MC}$ values vary by approximately 0.8 to 1.2-fold in the temperature range of 10.5–34.0°C. Based on the temperature-dependency of $k_{•OH,MC}$, the E_a values were calculated to be 11.6–13.1 kJ mol^{-1} by the Arrhenius plot (SI Figure S15b).

Ozonation of MCs in Natural Waters. The oxidative degradation of six MCs by ozonation was examined in two natural water samples (Maegok and Gamak). Different doses of O_3 (2–13 μM) were added into natural waters spiked with 0.1 μM MC, and the concentration of MC was measured following the reaction (Figures 2a–2f). Increasing the O_3 dose increased the degradation of MCs; 6 μM O_3 completely degraded MC-LW (which had the highest $k_{O3,MC}$), and approximately 10 μM O_3 was required for 90% degradation of other MCs. The degradation of MCs was lower in the Maegok water than in the Gamak water, because the Maegok water contains a higher concentration of DOC than the Gamak water (SI Table S3). DOC is a major consumer of oxidants (O_3 and $^{\bullet}OH$), thus decreasing the oxidant exposures.

The degradation of MCs by ozonation proceeds by the reactions of MCs with O_3 and $^{\bullet}OH$, and can be predicted by a simple kinetic model with the second-order rate constants ($k_{O3,MC}$ and $k_{\bullet OH,MC}$) and oxidant exposures (refer to equations 1 and 2).

$$d[MC]/dt = -k_{O3,MC}[O_3][MC] - k_{\bullet OH,MC}[^{\bullet}OH][MC] \quad (1)$$

$$[MC]_t = [MC]_0 \exp(-k_{O3,MC} \int[O_3]dt - k_{\bullet OH,MC} \int[^{\bullet}OH]dt) \quad (2)$$

The O_3 exposure ($\int[O_3]dt$) in natural water was calculated from the time-concentration profile of O_3 abatement measured by SFS (SI Table S4). The $^{\bullet}OH$ exposure ($\int[^{\bullet}OH]dt$) was calculated from the decomposition kinetics of a $^{\bullet}OH$ probe compound (*p*CBA) according to the following equation (SI Table S5).[40]

$$\int[^{\bullet}OH]dt = \ln([pCBA]_0/[pCBA]) / k_{\bullet OH,pCBA} \quad (3)$$

The calculated values of $\int[O_3]dt$ and $\int[^{\bullet}OH]dt$ in the two natural waters were plotted as a function of the O_3 input dose (Figures 3a and 3b). As anticipated, the oxidant exposures in the Maegok water (which contains a higher concentration of DOC) were lower than those in the Gamak water. Further, note that $\int[O_3]dt$ and $\int[^{\bullet}OH]dt$ exhibit exponential and linear increases with the O_3 dose, respectively, which is in agreement with the previous observations.[41,42] These observations indicate that the conversion of O_3 into $^{\bullet}OH$ is accelerated at lower doses of O_3. Using the kinetic equation with the determined $k_{O3,MC}$, $k_{\bullet OH,MC}$, $\int[O_3]dt$, and $\int[^{\bullet}OH]dt$ values (equation 2), the degradation of MCs was modeled (solid lines in Figures 2a–2f). For all MCs, the model predictions (solid lines) fit well with the experimental data (symbols), validating the rate constants determined in this study. The fractions of MCs degraded by the reactions of O_3 and $^{\bullet}OH$ were calculated so as to evaluate the contributions of the two oxidants (SI Figure S18). The contribution of O_3 generally dominated over that of $^{\bullet}OH$, accounting for 60−100% depending on the target MC and the O_3 dose.

Hepatotoxicity Change. The kinetic study in the previous section suggests that O_3 may primarily attack parts other than the Adda moiety for some MCs (e.g., the tyrosine and tryptophan moieties of MC-YR and MC-LW, respectively). This can lead to the formation of oxidation products with an intact Adda moiety which still retain hepatotoxicity. In order to test this possibility, the hepatotoxicity change in the MC-containing solution was monitored during the reaction with O_3, and the result was compared with the decrease in MC concentration (Figures 4a–4f).

For four MCs (MC-LR, -RR, -LA, and -LF), the decrease of the relative hepatotoxicity was almost proportional to the relative decrease of MC concentration (negligible or very small red areas in Figures 4a–4d), indicating that most of their oxidation products may have the transformed Adda moiety. However, for MC-YR and MC-LW, the decrease of hepatotoxicity was much lower than the decrease of concentration, particularly at lower O_3 doses (large red areas in Figures 4e and 4f), indicating that the primary oxidation products retain hepatotoxicity. At increased O_3 doses, the

hepatotoxicity was significantly decreased due to the oxidation of the Adda moiety. Indeed, the LC/MS analysis showed that the oxidation products with an intact Adda moiety are formed during the reactions of MC-YR and MC-LW with O_3 (the insets of Figures 4e and 4f); refer to the following section for details.

Oxidation Products of MCs. A product study using LC/MS was performed in order to examine the oxidation pathways of MCs by the reaction with O_3. The oxidation products were analyzed for the six MCs under the same conditions as those used for Figures 4a–4f. The major identified products are summarized in SI Table S6 (refer to Figures S19–S46 for their chromatograms). For the four MCs (MC-LR, -RR, -LA, and -LF), only two major products were identified (the peaks for other products were minor, and thereby not included in the table). Meanwhile, eight major products were identified for MC-YR and MC-LW. The oxidation pathways of MCs were postulated in accordance with the known ozonation chemistry based on these identified products (Figure 5).[43]

There are five sites in the target MC molecules that are considered to be primarily attacked by O_3 (Sites A–E): Two alkene groups in Adda (Sites A and B) and an alkene group in Mdha (Site C), a phenolic group in tyrosine (Site D for MC-YR), and an indolic double bond in tryptophan (Site E for MC-LW) (refer to Figure 1). The oxidation of MCs by O_3 can be successfully explained by four types of reactions (Reactions I–IV) initiated by the attack of O_3 on Sites A–E (Figure 5). The ozonation mechanisms known for the functional groups in Sites A–E can be described in detail as follows (refer to SI Figure S47). First, the ozone attack on alkenes generally proceeds according to the Criegee mechanism, yielding two carbonyl products through a cleavage of the C–C double bond[44] (SI Figure S47a): the electrophilic addition of O_3 initially forms an ozonide intermediate, which is rapidly decomposed into a carbonyl product and a carbonyl oxide (the carbonyl oxide is further transformed into a carbonyl product by hydrolysis). Second, the ozonation of phenol proceeds via dual routes, the ring-opening and the hydroxylation[45] (Reactions I and II in SI Figure S47b). The

hydroxylated product, dihydroxybenzene, can be further oxidized to benzoquinone[43] (Reaction III in SI Figure S47b). Third, the ozonation of tryptophan results in the cleavage of the indolic double bond to yield *N*-formylkynurenine (Reaction I in SI Figure S47c), which is subsequently transformed into kynurenine by acid hydrolysis (Reaction IV in SI Figure S47c).[46] The secondary reaction of kynurenine with O_3 yields aminophenol (Reaction II in SI Figure S47c).[42]

In the four MCs (i.e., MC-LR, -RR, -LA, and -LF), the oxidative cleavage of alkenes at Sites A and B produced aldehyde and ketone products via Reaction I (PLR1, PLR2, PRR1, PRR2, PLA1, PLA2, PLF1, and PLF2). All of these products have a damaged Adda moiety (Figure 5a); the primary products formed by the oxidation of Site C were not found. This observation is consistent with the fact that the second-order rate constants for the reactions of the four MCs with O_3 ($7.1–8.9 \times 10^5$ M^{-1} s^{-1}) are similar to that of sorbic acid ($k_{O3,sorbic\ acid} = 9.6 \times 10^5$ M^{-1} s^{-1} [24]), the model compound representing the Adda moiety of MCs. By contrast, the ozonation of MC-LW and -YR produced primary products with an intact Adda moiety due to the preferential oxidation of amino acids, tyrosine and tryptophan (for MC-YR and MC-LW, respectively) (Figures 5b and 5c). For MC-YR, the oxidation of the phenolic group at Site D by Reactions I and II produced ring-opened (PYR7) and hydroxylated (PYR6) products, respectively. The phenolic group in MC-YR exhibits higher reactivity with O_3 than the Adda moiety; $k_{O3,phenolic\ group}$ is estimated to be 1.2×10^6 M^{-1} s^{-1} at pH 7.8, which is higher than $k_{O3,sorbic\ acid}$ (9.6×10^5 M^{-1} s^{-1} [24]). PYR6 was further oxidized to a benzoquinone product (PYR5) by Reaction III. For MC-LW, the tryptophan moiety is primarily oxidized by O_3 ($k_{O3,tryptophan} = 7.0 \times 10^6$ M^{-1} s^{-1} [34]). The oxidation of the indolic double bond at Site E by Reaction I produced an *N*-formylkynurenine product (PLW6), which was subsequently transformed into a kynurenine product (PLW4) by Reaction IV. PLW4 and PLW6 were further oxidized to aminophenol products (PLW5 and PLW7, respectively) by Reaction II. Through extended oxidation, sites A and B in all of these products from MC-YR and MC-LW were oxidized by Reaction I, yielding a number of daughter products with a damaged Adda moiety (PYR1–4 and PLW1–3). The

signal intensities of oxidation products with an intact Adda moiety were presented for the ozonation of MC-YR and MC-LW at different O_3 doses (the insets of Figures 4e and 4f), which reasonably explained the gap between the MC concentration and the solution toxicity (the red areas in Figures 4e and 4f).

Practical Implications. This study reports the accurate values of $k_{O3,MC}$ and $k_{•OH,MC}$ for six major MCs (i.e., MC-LR, -RR, -LA, -LF, -YR, and -LW). Many of those values were reported here for the first time, while some of the values (e.g., those for MC-LR) were updated. The determined rate constants can be used to predict the removal of MCs by ozonation in the drinking water treatment process. Concentrations of dissolved MCs in natural waters has been reported up to 40 μg L^{-1}.[47,48] Assuming the highest MC concentration (40 μg L^{-1}), 99% of the initial MCs should be removed to meet the WHO guideline for drinking water (1 μg L^{-1} for MC-LR). Based on the results in this study, the specific O_3 doses required for 99% removal of MCs range from 0.06 to 0.18 g O_3 g DOC^{-1} depending on the MC congener (refer to SI Table S7). However, the decrease in toxicity of certain MCs (e.g., MC-YR and MC-LW) is not proportional to the decrease in concentration due to the occurrence of oxidation products with an intact Adda moiety. To minimize the risk of residual toxicity, increased O_3 doses need to be used to further destroy the Adda moiety in those oxidation products; the specific O_3 dose of 0.18 g O_3 g DOC^{-1} will be sufficient to completely remove the toxicity of MCs for typical natural water conditions (SI Figure S48).

Supporting Information Reagents (Text S1), $k_{O3,CA}$ determination (Text S2, Tables S1, S2, Figures S1, S3, and S4), temperature-dependent $k_{O3,pCBA}$ determination (Text S3 and Figure S6), correction for UV photolysis of MCs (Text S4), LC/MS analysis (Text S5), O_3 analysis in natural waters (Text S6 and Figure S10), water quality parameters of natural waters (Table S3), $\int[O_3]dt$ and $\int[•OH]dt$ values in natural waters (Tables S4 and S5), chromatograms and mass spectra of identified oxidation

products (Table S6 and Figures S19–S46), specific O_3 doses required for 99% removal of MCs in natural waters (Table S7), pH-dependent molar absorption coefficient of CA (Figure S2), example of CK plot for $k_{O3,MC\text{-}LR}$ (Figure S5), information about the photoreactor (Figure S7), measurement of incident UV intensity (Figure S8), a time-dependent profile of $\ln([H_2O_2]_0/[H_2O_2])$ during the UV/H_2O_2 experiment (Figure S9), pH and temperature-dependent $k_{O3,MC}$ and $k_{\bullet OH,MC}$ (Figure S11), CK plots for $k_{O3,MC}$ and $k_{\bullet OH,MC}$ at different O_3 doses, pHs, and temperatures (Figures S12, S13, S16 and S17), $k_{O3,MC\text{-}LR}$ determined by SFS (Figure S14), Arrhenius plots of $k_{O3,MC}$ and $k_{\bullet OH,MC}$ (Figure S15), contributions of O_3 and $^{\bullet}OH$ to the oxidation of MCs in natural waters (Figures S18), ozonation mechanisms (Figures S47), and changes of MC concentration and hepatotoxicity after ozonation in natural waters (Figure S48).

ACKNOWLEDGMENTS

This work was supported by the Korea Ministry of Environment as an "Advanced Industrial Technology Development Project" (2017000140005), and a National Research Foundation of Korea (NRF) Grant (NRF2017R1A2B3006827).

References

1. Watanabe, M. F.; Oishi, S.; Harada, K.-I.; Matsuura, K.; Kawai, H.; Suzuki, M. Toxins contained in Microcystis species of cyanobacteria (blue-green algae). *Toxicon* **1988**, *26* (11), 1017–1025.
2. Carmichael, W. W. Cyanobacteria secondary metabolites–the cyanotoxins. *J. Appl. Bacteriol.* **1992**, *72* (6), 445–459.
3. Matsushima, R.; Yoshizawa, S.; Watanabe, M. F.; Harada, K.-I.; Furusawa, M.; Carmichael, W. W.; Fujiki, H. In vitro and in vivo effects of protein phosphatase inhibitors, microcystins

and nodularin, on mouse skin and fibroblasts. *Biochem. Biophys. Res. Commun.* **1990**, *171* (2), 867–874.

4. Falconer, I. R. Tumor promotion and liver injury caused by oral consumption of cyanobacteria. *Environ. Toxicol. Water Qual.* **1991**, *6* (2), 177–184.
5. Dawson, R. M. The toxicology of microcystins. *Toxicon* **1998**, *36* (7), 953–962.
6. Hitzfeld, B. C.; Hoger, S. J.; Dietrich, D. R. Cyanobacterial toxins: Removal during drinking water treatment, and human risk assessment. *Environ. Health. Perspect.* **2000**, *108*, 113–122.
7. Sivonen, L.; Jones, G. In *Toxic Cyanobacteria in Water: A Guide to Public Health Significance, Monitoring and Management*; Chorous, I., Bartram, J., Eds.; E&FN Spon: London, 1999; p 41–111.
8. Theakston, R. D. G.; Reid, H. A. Development of simple standard assay procedures for the characterization of snake venoms. *Bull. World Health Organ.* **1983**, *61* (6), 949–956.
9. Jochimsen, E. M.; Carmichael, W. W.; An, J. S.; Cardo, D. M.; Cookson, S. T.; Holmes, C. E.; Antunes, M. B.; de Melo Filho D. A.; Lyra, T. M.; Barreto, V. S.; Azevedo, S. M.; Jarvis, W. R. Liver failure and death after exposure to microcystins at a hemodialysis center in *Brazil. New Engl. J. Med.* **1998**, *338* (13), 873–878.
10. Pouria, S.; de Andrade, A.; Barbosa, J.; Cavalcanti, R. L.; Barreto, V. T.; Ward, C. J.; Preiser, W.; Poon, G. K.; Neild, G. H.; Codd, G. A. Fatal microcystin intoxication in haemodialysis unit in Caruaru, Brazil. *Lancet* **1998**, *352* (9121), 21–26.
11. World Health Organization. *Guidelines for Drinking-Water Quality*, 4th ed.; World Health Organization: Geneva, 2011.
12. Carmichael, W. W.; Beasley, V.; Bunner, D. L.; Eloff, J. N.; Falconer, I.; Gorham, P.; Harada, K.-I.; Krishnamurthy, T.; Min-Juan, Y.; Moore, R. E.; Rinehart, K.; Runnegar, M.; Skulberg, O. M.; Watanabe, M. Naming of cyclic heptapeptide toxins of cyanobacteria (blue-green algae). *Toxicon* **1988**, *26* (11), 971–973.

13. Rinehart, K. L.; Namikoshi, M.; Choi, B. W. Structure and biosynthesis of toxins from blue-green algae (cyanobacteria). *J. Appl. Phycol.* **1994**, *6* (2), 159–176.
14. Graham, J. L.; Loftin, K. A.; Meyer, M. T.; Ziegler, A. C. Cyanotoxin mixtures and taste-and-odor compounds in cyanobacterial blooms from the Midwestern United States. *Environ. Sci. Technol.* **2010**, *44* (19), 7361–7368.
15. Faassen, E. J.; Lürling, M. Occurrence of the microcystins MC-LW and MC-LF in Dutch surface waters and their contribution to total microcystin toxicity. *Mar. Drugs* **2013**, *11* (7), 2643–2654.
16. Puddick, J.; Prinsep, M. R.; Wood, S. A.; Kaufononga, S. A. F.; Cary, S. C.; Hamilton, D. P. High levels of structural diversity observed in microcystins from *Microcystis* CAWBG11 and characterization of six new microcystin congeners. *Mar. Drugs* **2014**, *12* (11), 5372–5395.
17. von Gunten, U. Ozonation of drinking water: Part I. Oxidation kinetics and product formation. *Water Res*. **2003**, *37* (7), 1443–1467.
18. Buxton, G. V.; Greenstock, C. L.; Helman, W. P.; Ross, A. B. Critical review of rate constants for reactions of hydrated electrons, hydrogen atoms and hydroxyl radicals ($^{\bullet}OH/^{\bullet}O^{-}$) in aqueous solution. *J. Phys. Chem. Ref. Data* **1988**, *17* (2), 513–886.
19. Huber, M. M.; Canonica, S.; Park, G.-Y.; von Gunten, U. Oxidation of pharmaceuticals during ozonation and advanced oxidation processes. *Environ. Sci. Technol*. **2003**, *37* (5), 1016–1024.
20. Rositano, J.; Nicholson, B. C.; Pieronne, P. Destruction of cyanobacterial toxins by ozone. *Ozone Sci. Eng.* **1998**, *20* (3), 223–238.
21. Rositano, J.; Newcombe, G.; Nicholson, B.; Sztajnbok, P. Ozonation of NOM and algal toxins in four treated waters. *Water Res.* **2001**, *35* (1), 23–32.
22. Shawwa, A. R.; Smith, D. W. Kinetics of microcystin-LR oxidation by ozone. *Ozone Sci. Technol*. **2001**, *23* (2), 161–170.

385 23. Brooke, S.; Newcombe, G.; Nicholson, B.; Klass, G. Decrease in toxicity of microcystins LA
386 and LR in drinking water by ozonation. *Toxicon* **2006**, *48* (8), 1054–1059.
387 24. Onstad, G. D.; Strauch, S.; Meriluoto, J.; Codd, G. A.; von Gunten, U. Selective oxidation of
388 key functional groups in cyanotoxins during drinking water ozonation. *Environ. Sci. Technol.*
389 **2007**, *41* (12), 4397–4404.
390 25. Al Momani, F. A.; Jarrah, N. Treatment and kinetic study of cyanobacterial toxin by ozone, *J.*
391 *Environ. Sci. Health A* **2010**, *45* (6), 719–731.
392 26. Miao, H.-F.; Qin, F.; Tao, G.-J.; Tao, W.-Y.; Ruan, W. -Q. Detoxification and degradation of
393 microcystin-LR and -RR by ozonation. *Chemosphere* **2010**, *79* (4), 355–361.
394 27. Chang, J.; Chen, Z.-L.; Wang, Z.; Shen, J.-M.; Chen, Q.; Kang, J.; Yang, L.; Liu, X.-W.; Nie,
395 C.-X. Ozonation degradation of microcystin-LR in aqueous solution: Intermediates,
396 byproducts and pathways. *Water Res.* **2014**, *63*, 52–61.
397 28. Svrcek, C.; Smith, D. W. Cyanobacteria toxins and the current state of knowledge on water
398 treatment options: A review. *J. Environ. Eng. Sci.* **2004**, *3* (3), 155–185.
399 29. Leitzke, A.; Reisz, E.; Flyunt, R.; von Sonntag, C. The reactions of ozone with cinnamic acid:
400 Formation and decay of 2-hydroperoxy-2-hydroxyacetic acid. *J. Chem. Soc., Perkin Trans. 2*
401 **2001**, *5*, 793–797.
402 30. Wolf, C.; von Gunten, U.; Kohn, T. Kinetics of inactivation of waterborne enteric viruses by
403 ozone. *Environ. Sci. Technol.* **2018**, *52* (4), 2170–2177.
404 31. Jans, U. Radikalbildung aus Ozon in atmosphärischen Wassern Einfluss von Licht, gelösten
405 Stoffen and Russpartikeln. Doctoral Thesis, ETH Zurich, 1996.
406 32. Neta, P.; Dorfman, L. M. Pulse radiolysis sduties. XIII. Rate constants for the reaction of
407 hydroxyl radicals with aromatic compounds in aqueous solutions. In *Advances in Chemistry,*
408 *Radiation Chemistry*; American Chemical Society, 1968; Vol. *81*, pp 222–230.
409 33. Hatchard, C. G.; Parker, C. A. A new sensitive chemical actinometer. II. Potassium

410 ferrioxalate as a standard chemical actinometer. *Proc. Roy. Soc. Lond. Ser. Math. Phys. Sci.*
411 **1956**, *235* (1203), 518–536.
412 34. Pryor, W. A.; Giamalva, D. H.; Church, D. F. Kinetics of ozonation. 2. Amino acids and
413 model compounds in water and comparisons to rates in nonpolar solvents. *J. Am. Chem. Soc.*
414 **1984**, *106* (23), 7094–7100.
415 35. Hoigné, J.; Bader, H. Rate constants of reactions of ozone with organic and inorganic
416 compounds in water–II. *Water Res.* **1983**, *17* (2), 185–194.
417 36. Dowideit, P.; von Sonntag, C. Reaction of ozone with ethene and its methyl- and chlorine-
418 substituted derivatives in aqueous solution. *Environ. Sci. Technol.* **1998**, *32* (8), 1112–1119.
419 37. Robarts, R. D.; Zohary, T. Temperature effects on photosynthetic capacity respiration, and
420 growth rates of bloom-forming cyanobacteria. *New Zeal. J. Mar. Fresh. Res.* **1987**, *21* (3),
421 391–399.
422 38. He, X.; Pelaez, M.; Westrick, J. A.; O'Shea, K. E.; Hiskia, A.; Triantis, T.; Kaloudis, T.;
423 Stefan, M. I.; de la Cruz, A. A.; Dionysiou, D. D. Efficient removal of microcystin-LR by
424 UV/H_2O_2 in synthetic and natural water samples. *Water Res.* **2012**, *46* (5), 1501–1510.
425 39. Song, W.; Xu, T.; Cooper, W. J.; Dionysiou, D. D.; de la Cruz, A. A.; O'Shea, K. E.
426 Radiolysis studies on the destruction of microcystin-LR in aqueous solution by hydroxyl
427 radicals. *Environ. Sci. Technol.* **2009**, *43* (5), 1487–1492.
428 40. Elovitz, M. S.; von Gunten, U. Hydroxyl radical/ozone ratios during ozonation processes. I.
429 The R_{ct} concept. *Ozone Sci. Eng.* **1999**, *21* (3), 239–260.
430 41. Lee, Y.; Gerrity, D.; Lee, M.; Bogeat, A. E.; Salhi, E.; Gamage, S.; Trenholm, R. A.; Wert, E.
431 C.; Snyder, S. A.; von Gunten, U. Prediction of micropollutant elimination during ozonation
432 of municipal wastewater effluents: Use of kinetic and water specific information. *Environ. Sci.*
433 *Technol.* **2013**, *47* (11), 5872–5881.

42. Lee, Y.; von Gunten, U. Advances in predicting organic contaminant abatement during ozonation of municipal wastewater effluent: Reaction kinetics, transformation products, and changes of biological effects. *Environ. Sci.: Water Res. Technol.* **2016**, *2*, 421–442.
43. Bailey, P. S. *Ozonation in Organic Chemistry*; Academic Press: New York, 1982; Vol. *2*.
44. Criegee, R. Mechanism of ozonolysis. *Angew. Chem. Int. Ed.* **1975**, *14* (11), 745–752.
45. Yamamoto, Y.; Niki, E.; Shiokawa, H.; Kamiya, Y. Ozonation of organic compounds. 2. Ozonation of phenol in water. *J. Org. Chem.* **1979**, *44* (13), 2137–2142.
46. Cataldo, F. On the action of ozone on proteins. *Polym. Degrad. Stabil.* **2003**, *82* (1), 105–114.
47. Oh, H.-M.; Lee, S. J.; Kim, J. -H.; Kim, H.-S.; Yoon, B.-D. Seasonal variation and indirect monitoring of microcystin concentrations in Daechung reservoir, Korea. *Appl. Environ. Microbiol.* **2001**, *67* (4), 1484–1489.
48. Bláhová, L.; Babica, P.; Maršálková, E.; Maršálek, B.; Bláha, L. Concentrations and seasonal trends of extracellular microcystins in freshwaters of the Czech republic – Results of the national monitoring program. *Clean: Soil, Air, Water* **2007**, *35* (4), 348–354.

Table 1. Summary of $k_{O3,MC}$ (and $k_{O3,CA}$) and $k_{\bullet OH,MC}$, and E_a values

	MC-LR	MC-RR	MC-LA	MC-LF	MC-YR	MC-LW	CA	Conditions	References
$k_{O3,MC}$ ($k_{O3,CA}$) ($\times 10^5$ M^{-1} s^{-1})							7.6	pH 7, 22°C	30
	0.3							pH 7, 20°C	22
	0.7	2.5						pH 7, 20°C	25
	4.1 ± 0.1[a]						3.8[b]	pH 8, 20−21°C	24, 29
	8.5 ± 0.2	8.9 ± 0.1	8.0 ± 0.2	7.1 ± 0.1	8.6 ± 0.1[c] 1490[d]	61.2 ± 1.6	7.8 ± 0.1	pH 7.2, 20 ± 1°C	This study
E_a for $k_{O3,MC}$ ($k_{O3,CA}$) (kJ mol^{-1})							21.2 ± 0.7	pH 7, 2−22°C	30
	12.3							pH 7, 10−30°C	22
	24.7 ± 0.7	27.5 ± 0.1	32.9 ± 1.4	21.6 ± 0.2	34.5 ± 0.5	29.0 ± 0.9	19.1 ± 1.2	pH 7.2, 4−33°C	This study
$k_{\bullet OH,MC}$ ($\times 10^{10}$ M^{-1} s^{-1})	1.1							pH 8	24
	2.3 ± 0.1							pH 7, room temperature	39
	1.1	1.5	1.1		1.6			pH 7.4, 21 ± 1°C	38
	1.2 ± 0.1	1.4 ± 0.1	1.2	1.4	1.4 ± 0.2	1.8 ± 0.2		pH 7.2, 20 ± 1°C	This study
E_a for $k_{\bullet OH,MC}$ (kJ mol^{-1})	11.6 ± 0.7	11.9 ± 0.8	12.5 ± 0.1	13.1 ± 0.5	12.2 ± 0.3	11.6 ± 0.2		pH 7.2, 5.6−38.1°C	This study

[a]Ref 24. [b]Ref 29. [c]$k_{O3,MC\text{-}YR(HA)}$, and [d]$k_{O3,MC\text{-}YR(A-)}$; pK_a of phenolic group in MC-YR = 9.9.

Figure Captions

Figure 1. (a) Structure of MC skeleton and (b) L-amino acids located in the X and Y positions for the six MCs (MC-LR, -RR, -LA, -LF, -YR, and -LW). Primary oxidation sites (A–E) are highlighted in red areas.

Figure 2. Oxidation of MCs by ozonation in natural waters. Symbols and lines represent experimental data and model predictions, respectively ($[MCs]_0$ = 0.1 μM, 20 ± 1°C).

Figure 3. Exposures of (a) O_3 and (b) $^{\bullet}OH$ at different input doses of O_3 in natural waters (20 ± 1°C).

Figure 4. Changes of MC concentration and hepatotoxicity by reaction with O_3 at different doses. Insets of (e) and (f) represent the LC/MS signal intensity for oxidation products with an intact Adda moiety ($[MCs]_0$ = 0.1 μM, $[t\text{-BuOH}]_0$ = 5 mM, pH = 7.8, temperature = 20 ± 1°C).

Figure 5. Proposed pathways for the oxidation of MCs by O_3.

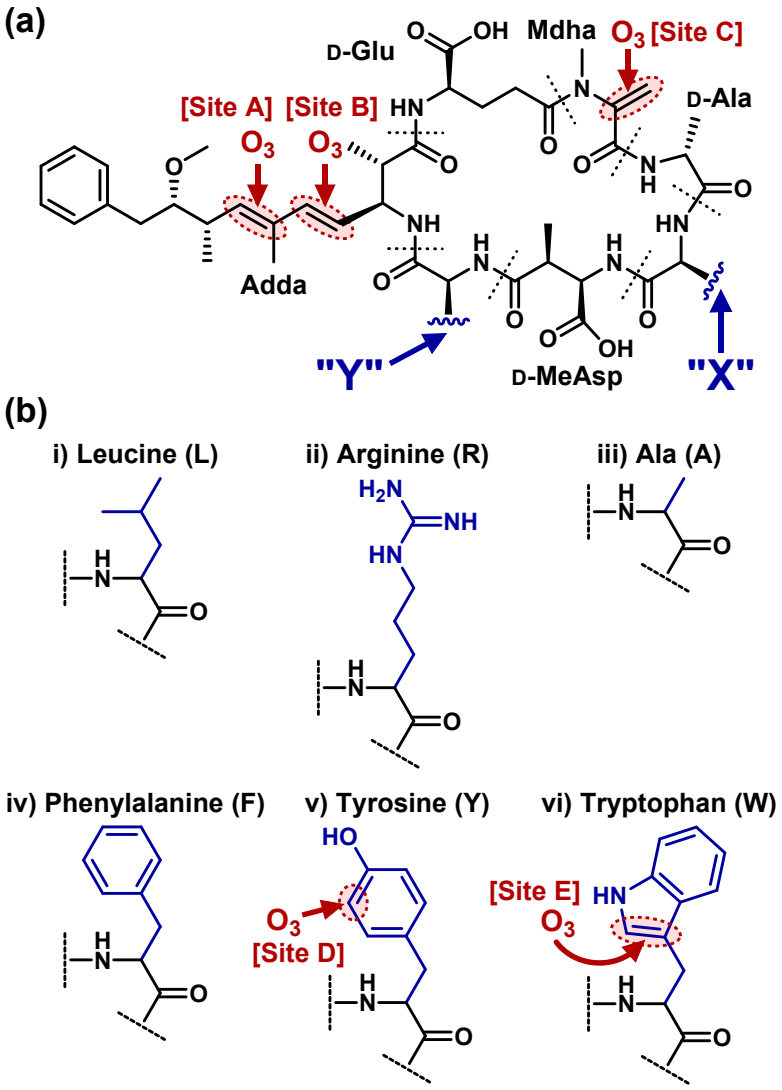
(a)
D-Glu
Mdha
O3 [Site C]
D-Ala
[Site A]
[Site B]
O3
O3
Adda
"Y"
D-MeAsp
"X"
(b)
i) Leucine (L)
ii) Arginine (R)
iii) Ala (A)
iv) Phenylalanine (F)
v) Tyrosine (Y)
vi) Tryptophan (W)
O3
[Site D]
[Site E]
O3

Figure 1.

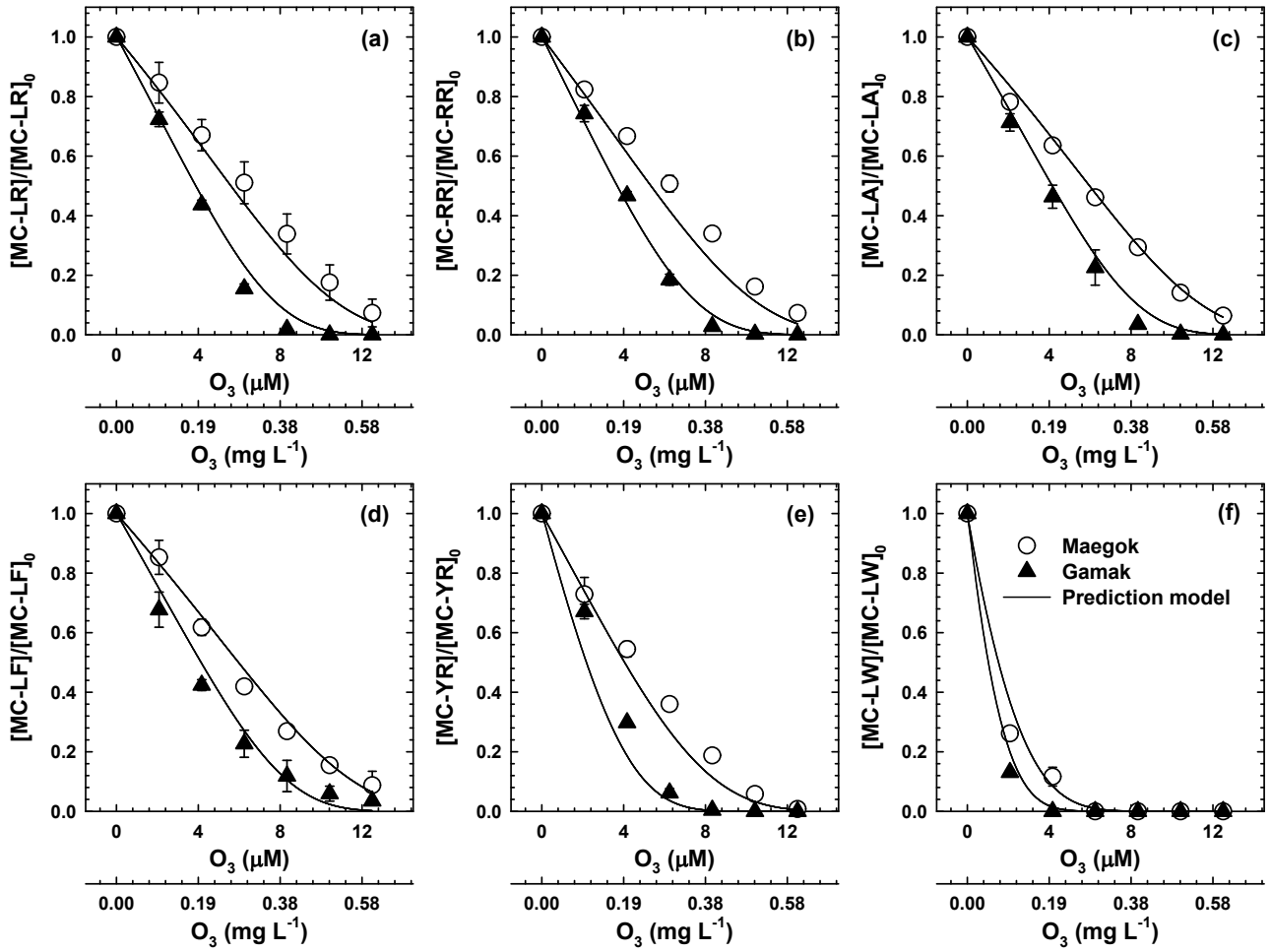
(a)
(b)
(c)
(d)
(e)
(f)
[MC-LR]/[MC-LR]0
[MC-RR]/[MC-RR]0
[MC-LA]/[MC-LA]0
[MC-LF]/[MC-LF]0
[MC-YR]/[MC-YR]0
[MC-LW]/[MC-LW]0
O3 (μM)
O3 (mg L-1)
Maegok
Gamak
Prediction model

Figure 2.

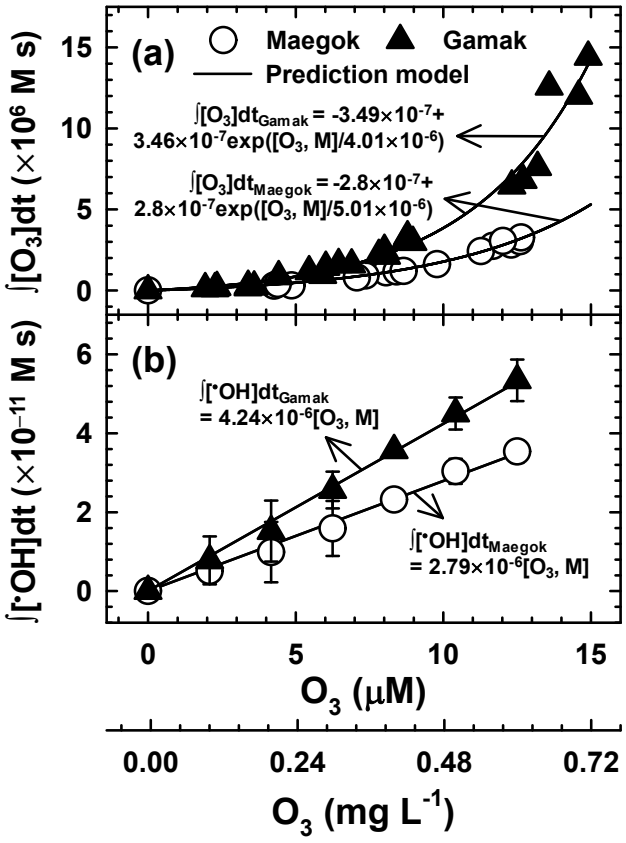
(a)
Maegok
Gamak
Prediction model
∫[O3]dtGamak = -3.49×10-7+ 3.46×10-7exp([O3, M]/4.01×10-6)
∫[O3]dtMaegok = -2.8×10-7+ 2.8×10-7exp([O3, M]/5.01×10-6)
∫[O3]dt (×10^6 M s)
(b)
∫[•OH]dtGamak = 4.24×10-6[O3, M]
∫[•OH]dtMaegok = 2.79×10-6[O3, M]
∫[•OH]dt (×10^-11 M s)
O3 (μM)
O3 (mg L-1)

Figure 3.

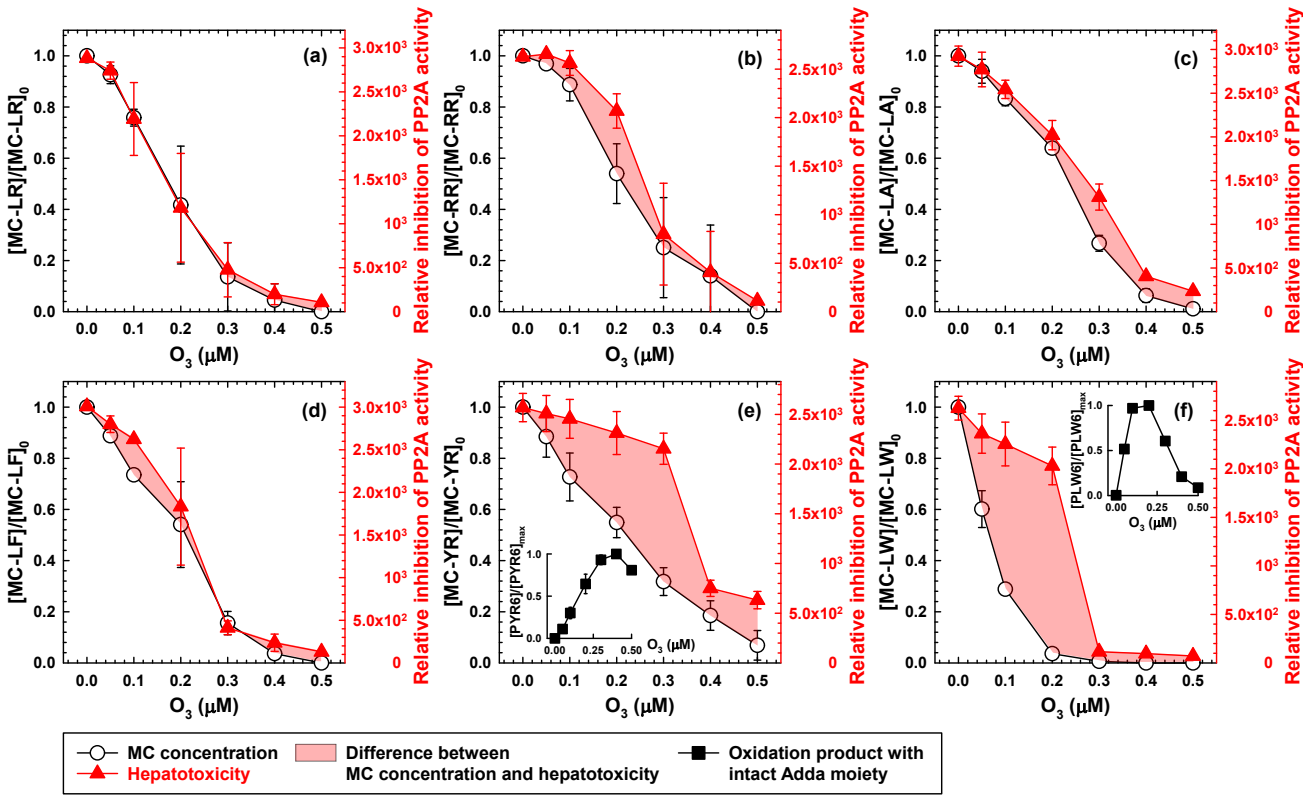
(a)
(b)
(c)
(d)
(e)
(f)
[MC-LR]/[MC-LR]0
[MC-RR]/[MC-RR]0
[MC-LA]/[MC-LA]0
[MC-LF]/[MC-LF]0
[MC-YR]/[MC-YR]0
[MC-LW]/[MC-LW]0
O3 (μM)
Relative inhibition of PP2A activity
[PYR6]/[PYR6]max
[PLW6]/[PLW6]max
MC concentration
Hepatotoxicity
Difference between MC concentration and hepatotoxicity
Oxidation product with intact Adda moiety

Figure 4.

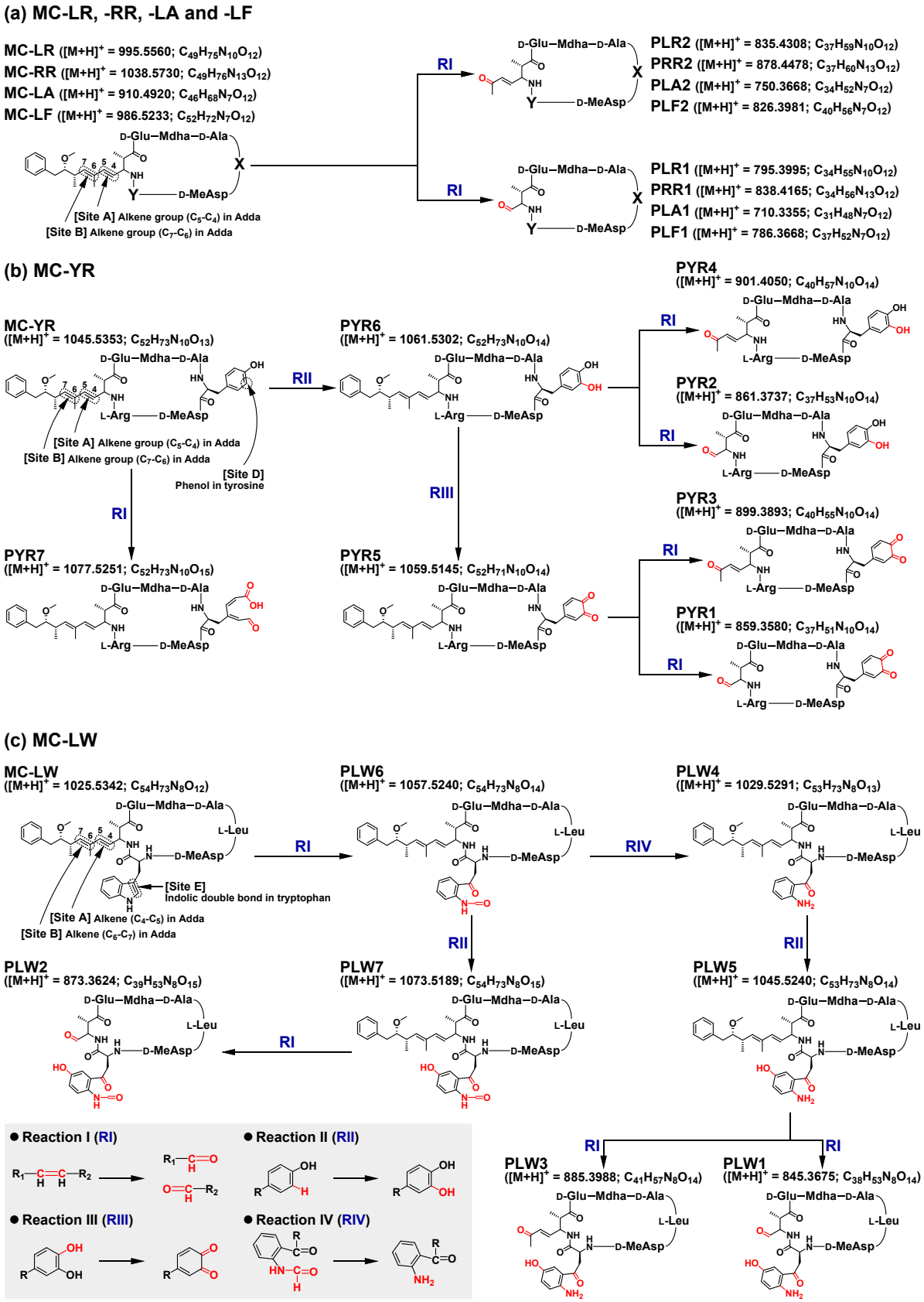
(a) MC-LR, -RR, -LA and -LF
MC-LR ([M+H]+ = 995.5560; C49H75N10O12)
MC-RR ([M+H]+ = 1038.5730; C49H76N13O12)
MC-LA ([M+H]+ = 910.4920; C46H68N7O12)
MC-LF ([M+H]+ = 986.5233; C52H72N7O12)
[Site A] Alkene group (C5-C4) in Adda
[Site B] Alkene group (C7-C6) in Adda
RI
PLR2 ([M+H]+ = 835.4308; C37H59N10O12)
PRR2 ([M+H]+ = 878.4478; C37H60N13O12)
PLA2 ([M+H]+ = 750.3668; C34H52N7O12)
PLF2 ([M+H]+ = 826.3981; C40H56N7O12)
PLR1 ([M+H]+ = 795.3995; C34H55N10O12)
PRR1 ([M+H]+ = 838.4165; C34H56N13O12)
PLA1 ([M+H]+ = 710.3355; C31H48N7O12)
PLF1 ([M+H]+ = 786.3668; C37H52N7O12)
(b) MC-YR
MC-YR ([M+H]+ = 1045.5353; C52H73N10O13)
[Site D] Phenol in tyrosine
RII
PYR6 ([M+H]+ = 1061.5302; C52H73N10O14)
PYR4 ([M+H]+ = 901.4050; C40H57N10O14)
PYR2 ([M+H]+ = 861.3737; C37H53N10O14)
RIII
PYR7 ([M+H]+ = 1077.5251; C52H73N10O15)
PYR5 ([M+H]+ = 1059.5145; C52H71N10O14)
PYR3 ([M+H]+ = 899.3893; C40H55N10O14)
PYR1 ([M+H]+ = 859.3580; C37H51N10O14)
(c) MC-LW
MC-LW ([M+H]+ = 1025.5342; C54H73N8O12)
[Site E] Indolic double bond in tryptophan
[Site A] Alkene (C4-C5) in Adda
[Site B] Alkene (C6-C7) in Adda
PLW6 ([M+H]+ = 1057.5240; C54H73N8O14)
PLW4 ([M+H]+ = 1029.5291; C53H73N8O13)
RIV
PLW2 ([M+H]+ = 873.3624; C39H53N8O15)
PLW7 ([M+H]+ = 1073.5189; C54H73N8O15)
PLW5 ([M+H]+ = 1045.5240; C53H73N8O14)
PLW3 ([M+H]+ = 885.3988; C41H57N8O14)
PLW1 ([M+H]+ = 845.3675; C38H53N8O14)
Reaction I (RI)
Reaction II (RII)
Reaction III (RIII)
Reaction IV (RIV)

Figure 5.